scientific reports

Check for updates

OPEN

# High resolution multiple scenario simulations of future extreme sea levels in hong kong and socioeconomic risks

Zhang Chen[1], Sicheng Jiang[1], Xindan Liang[1] & Hongsheng Zhang[1,2]✉

**Extreme sea levels (ESLs) induce significant risks to Hong Kong. With climate change, the risks will be amplified, while existing studies have not provided fine-grained simulations of Hong Kong's future ESL exposure and its socio-economic risks. Employing a GIS-based coastal flood inundation model, this research integrates a high-resolution Digital Terrain Model (DTM) with datasets of ESL forecasts, demography, economy, infrastructure, and land use to estimate the future ESL risks posed on Hong Kong for 2050 and 2100 under two Representative Concentration Pathways (RCPs): RCP4.5 and RCP8.5. The projections indicate that, under RCP4.5, over 27.66% of the population and 39.52% of the Gross Domestic Product (GDP) will be exposed to ESL after 2050. Under RCP8.5 scenario, the exposed population may surpass 31.21%, with economic exposure estimated at 40.98% of GDP after 2050. Under both RCPs, Hong Kong's ESL-threatened area may range from 8.23 to 11.41%, exposing over 16.09% of the infrastructure to ESL after 2050. Regions in the northwestern Yuen Long, Tuen Mun River Estuary, Rambler Channel coast, Victoria Harbor coast, Shing Mun River, and Tai Po Waterfront have particularly high ESL risks. The findings highlight the need for resilient infrastructure to counteract the long-term risks ESL poses in Hong Kong.**

**Keywords** Extreme sea levels, Coastal flooding, Urban vulnerability, High-resolution digital terrain model, Socio-economic impact projections

Extreme Sea Levels (ESLs) can directly lead to coastal flooding. ESLs can arise from the simultaneous occurrence of high astronomical tides, storm surges, and wind waves. These elements can be exacerbated by climate extremes such as typhoons, which synergistically contribute to extremely high sea levels. Typically, the return period of the ESLs we focus on is defined as 100 years[1,2]. ESLs are measured as the aggregated elevation resulting from mean sea level (MSL), storm surge, wind waves, and astronomical high tide. ESL events, though infrequent, have the potential to overtop coastal protective infrastructure, leading to coastal floods that severely impact the livelihoods of coastal environments, populations and the development of the local economy[3–5]. Therefore, it is considered a major natural threat to coastal zones, coastal communities, and economies[6,7].

In the context of climate change, ESL is expected to have a high possibility of increasing continuously. Data from global tide gauges imply that global ESL has increased since 1970, and the growth rate is accelerating[8]. In terms of future scenarios, projections indicate an upward trajectory in MSL and a concomitant intensification of storm surges[9,10]. The upward changes in these elements will consequently intensify future ESL events. Climate change is expected to amplify the frequency of ESL events[8]. Furthermore, the future coastal urban expansion may lead to the concentration of population and economic activities in coastal zones, especially the low-lying land, increasing the socio-economic vulnerabilities to ESL and amplifying the risks to societal development[8,11,12]. Given the escalating intensity of future ESL and the densification of coastal populations, coastal communities require a comprehensive analysis of ESL risks and their potential threats to enhance hazard prevention abilities.

Groups of studies have contributed to the field of ESL forecasting and modeling the potential threats of future ESL to coastal zones. Vousdoukas et al. provided a global-scale probability projection of future ESL[2]. Regarding ESL's impact on coastal lands, multiple existing research projects estimated the global-scale land, population, and economic exposure to future ESL[13–15]. Despite multitudinous research pertinent to the global-scale future ESL risk, localized studies are still in demand because global studies lack the granularity necessary for considering existing coastal flood prevention infrastructure[14]. Additionally, global studies are argued to be ineffective in

[1]Department of Geography, The University of Hong Kong, Pok Fu Lam, Hong Kong SAR, China. [2]The University of Hong Kong Shenzhen Institute of Research and Innovation, Shenzhen, China. ✉email: zhanghs@hku.hk

conferring the localized and community-scale ESL hazards, as local studies can better contextualize the risks to better incorporate the knowledge of ESL into local residents' lives[16,17].

In the field of local-scale ESL risk projections, current studies focus on the coastal cities in North America and Europe[1,6,12,18,19]. Recent studies also pay more and more attention to ESL-related risks in the Asia–Pacific region. Zheng et al. assessed ESL variations for island nations in the tropical western Pacific under different climate scenarios[20]. Kato and Tajima also reviewed Japan's responses to ESL hazards and the associated future challenges[21]. Hong Kong, as an Asian coastal megacity with a dense population and economic activities, has been historically exposed to ESL threats and suffered severe socioeconomic losses[3].

Some indirect evidence can imply that the ESL risks in Hong Kong are potentially increasing. The local mean sea level of Hong Kong has risen 2.9 mm annually from 1954 to 2013[22]. Compared to the period from 1986 to 2005, the MSL between 2018 and 2100 is expected to increase by 0.84 m under the current emission situation[22]. Regarding the storm surge strength, the hydrological events caused by tropical cyclones in Hong Kong became more intensive[23]. The projected upward tendencies of MSL, high tide height, and storm surge strength may jointly contribute to more destructive ESL events and threaten more population and economic activities in Hong Kong. In terms of ESL frequency, according to historical tide gauge station data of Hong Kong, the number of days with ESL events also showed significant growth during the past decades[3]. This evidence indirectly suggests that ESL risks in Hong Kong will increase in the coming decades.

However, while global-scale and city-level studies on ESL projection abound, there is a conspicuous dearth of research focusing specifically on ESL risks in Hong Kong, a coastal megacity. About 4.5 million residents reside in the coastal land reclamation zones, and more than 50% of its urban areas are located on coastal lowlands[24,25]. These factors make Hong Kong highly susceptible to rising sea levels and ESL events and may amplify socio-economic losses during ESL events. Additionally, the future ESL risks posed to Hong Kong's land, economy, and society have not been quantified on a local scale. This gap underscores the necessity for localized estimations of future ESL risks posed to the socio-economic development in the context of Hong Kong to inform targeted and effective urban planning and infrastructure development strategies. The elevation and location of Hong Kong are shown in Fig. 1. In addition, Fig. 1 also shows the location of the Quarry Bay Tide Gauge Station. The sea level data in this station is used to represent the mean sea level of Hong Kong and will be referred to later in the following section.

Our study endeavors to bridge this research gap by providing a high-resolution, multi-faceted estimation of the socio-economic risks of future ESL in Hong Kong. This study utilized a GIS-based coast flood model to combine a high-resolution Digital Terrain Model (DTM) of Hong Kong and multi-scenario projections of future ESLs to estimate Hong Kong's land area exposed to future ESLs. The ESL projections used in this study were produced by Vousdoukas et al.[2]. Their components include future mean sea levels, projected astronomical high tides, storm surges, and setups from wind waves during future extreme events. These components were projected based on scenarios in 2050 and 2100 under two Representative Concentration Pathways (RCPs), including RCP4.5 and RCP8.5.

The process used the ESL projections in 2050 and 2100 under both RCP4.5 and RCP8.5 scenarios to model four possible ESL cases. Based on the flood modeling results, we assessed the population, GDP, and infrastructure exposed to future ESL in Hong Kong. The land use composition in the ESL-threatened areas was also analyzed for each situation. This study aimed to reveal increasing socio-economic exposure to future ESL in Hong Kong. It also identified key areas with high ESL risks, highlighting the urgent need for informed urban resilience planning in the face of escalating ESL risks.

## Results

### Lands threatened by extreme sea levels

Visualization of land areas susceptible to future ESLs across all scenarios is provided in Fig. 2. Figure 2 reveals that the northwestern corner of Yuen Long District and the regions adjacent to Victoria Harbor are particularly prone to future ESLs because most of the lands in these regions are exposed to ESL risk in all RCP-year settings. The quantification of land areas at risk is depicted in Fig. 2, detailing that under RCP4.5, an estimated 91.68 $km^2$( 8.23%) of Hong Kong's land will face ESL exposure in 2050. The number will escalate to 105.83 $km^2$( 9.50%) by 2100. For the RCP8.5 scenario, the area at risk encompasses 101.82 $km^2$( 9.14%) in 2050, expanding to 127.11 $km^2$, equating to 11.41% of the territory by 2100.

Furthermore, Fig. 3 illustrates the maps and statistics related to the maximum possible inundation depth from ESL. The average maximum inundation depth in 2050, under RCP4.5, is projected to be 1.79 m, increasing to 1.90 m by 2100. Under the RCP8.5 scenario, the anticipated average maximum inundation will rise from 1.86 m in 2050 to 2.09 m in 2100. Notably, the northwestern corner of Yuen Long District, including the Mai Po Nature Reserve and surrounding resident areas, is expected to have a large tract of land exposed to ESL with possibly deep floods due to topographical factors, as highlighted in Fig. 3 using the simulation of maximum possible ESL inundation depth in 2100 under RCP8.5.

### Socio-economic risks of extreme sea levels

*ESL risks on population*

Figure 4 visualizes the projected population distribution within ESL risk zones for each scenario. The pertinent statistics are also compiled in the bar charts. Under the RCP4.5 scenario, 2.22 million individuals are projected to be at risk in 2050, constituting 27.66% of the projected total population of 8.03 million. By 2100, this figure adjusts to 1.60 million people, representing a percentage of 32.89%. Under RCP8.5, the population at risk is expected to be 2.51 million in 2050 (31.21%) and 1.96 million (40.41%) in 2100. It is observed that while the absolute number of individuals exposed to ESL decreases from 2050 to 2100 under the same RCP, the proportionate risk increases. This trend is attributed to the projected demographic shifts. The population is forecasted to decrease

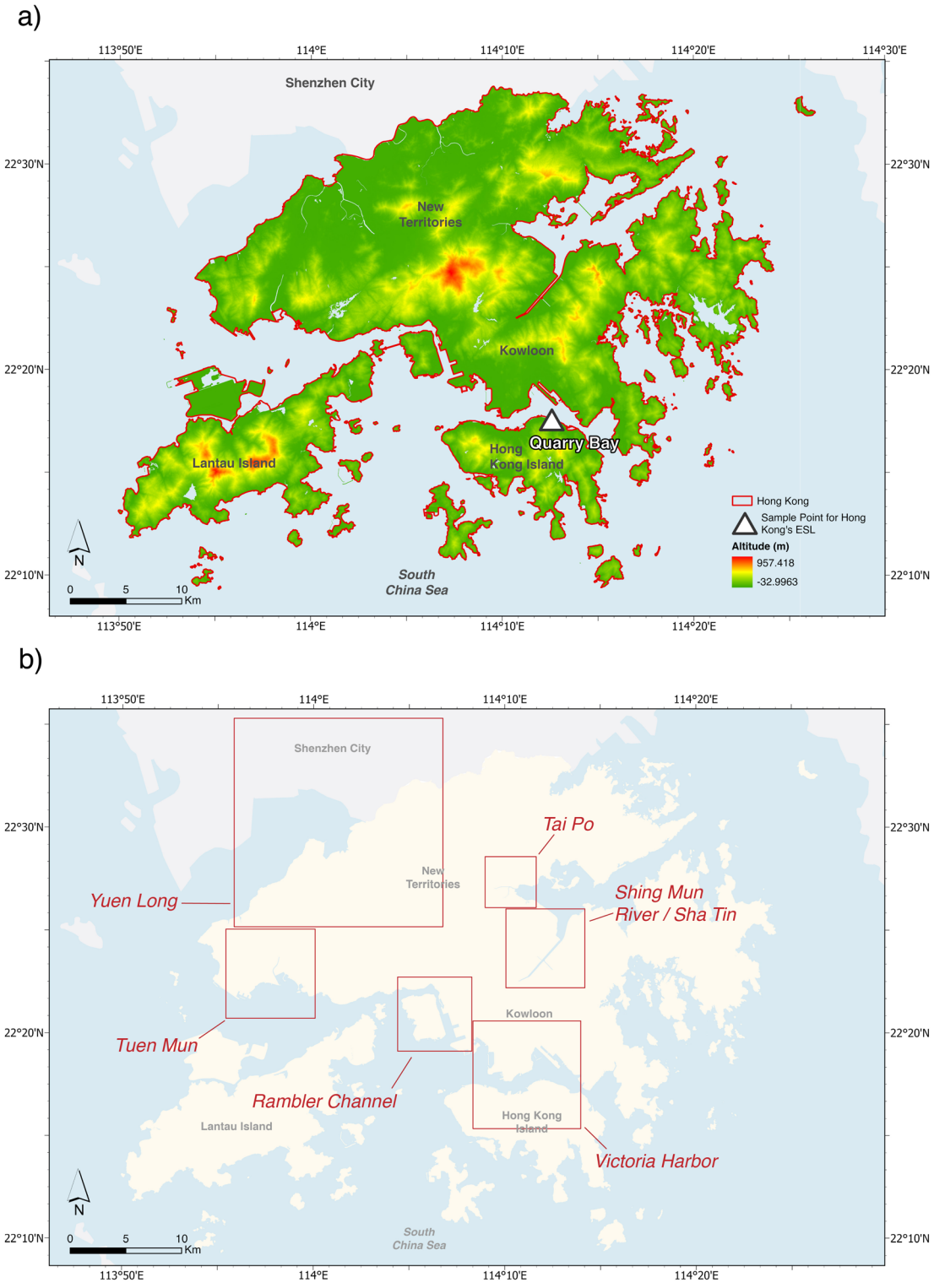


**Fig. 1**. (**a**) Location and terrain of the study area, Hong Kong, with the sample point for Hong Kong's ESL shown; (**b**) The locations and approximate extents of the areas mentioned in this study. The maps were created using ArcGIS Pro V3.4 by ESRI, which can be accessed from https://www.esri.com/en-us/arcgis/products/arcgis-pro/.

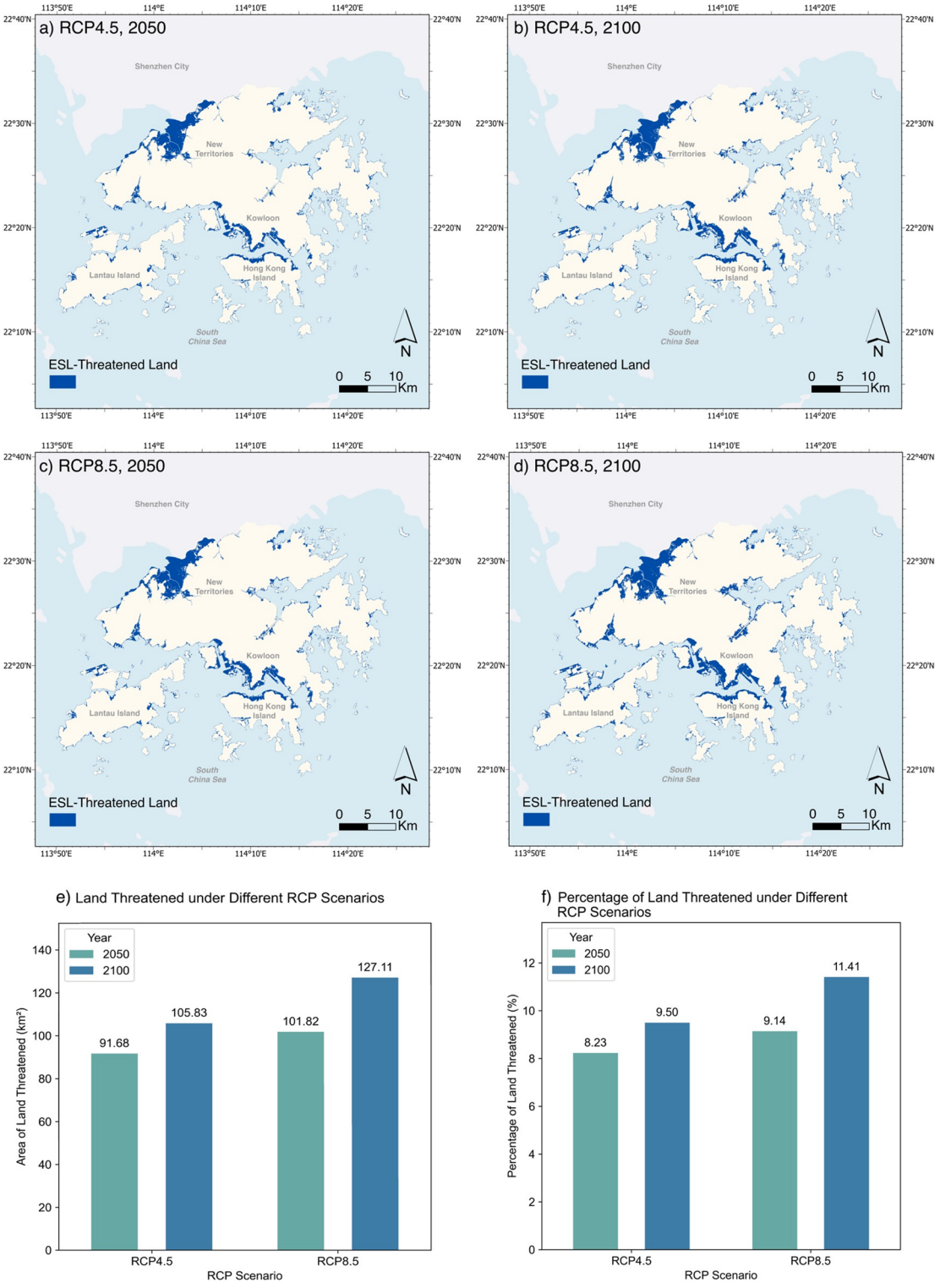


**Fig. 2**. (**a**-**d**) Maps of Hong Kong's lands exposed to ESL in different scenarios and years; (**e**) Bar chart of areas of ESL-threatened lands; (**f**) Bar chart of percentages of ESL-threatened lands. The maps were created using ArcGIS Pro V3.4 by ESRI, which can be accessed from https://www.esri.com/en-us/arcgis/products/arcgis-pro/.

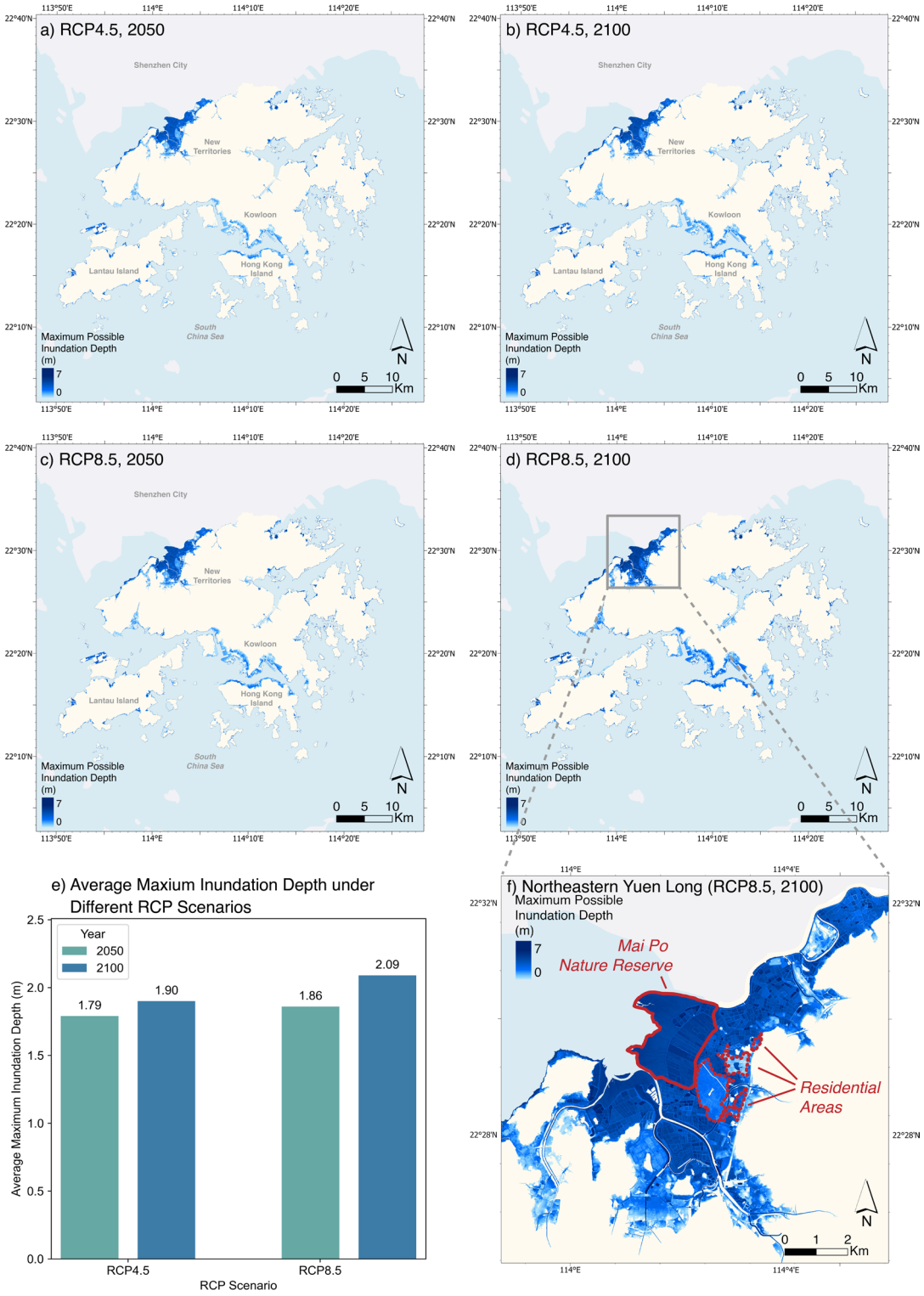


**Fig. 3**. (**a**-**d**) Maximum possible ESL inundation depths in Hong Kong in different scenarios and years; (**e**) Bar chart of Maximum possible ESL inundation depths in Hong Kong in different scenarios and years; (**f**) Maximum possible ESL inundation in the northeastern Yuen Long in the case of RCP8.5 in 2100. This region may be exposed to a vast and deep ESL inundation as it has a large wetland area and low-lying fishponds (Gai Wais). The locations and extents of the Mai Po Nature Reserve and its surrounding residential areas are highlighted. The maps were created using ArcGIS Pro V3.4 by ESRI, which can be accessed from https://www.esri.com/en-us/arcgis/products/arcgis-pro/.

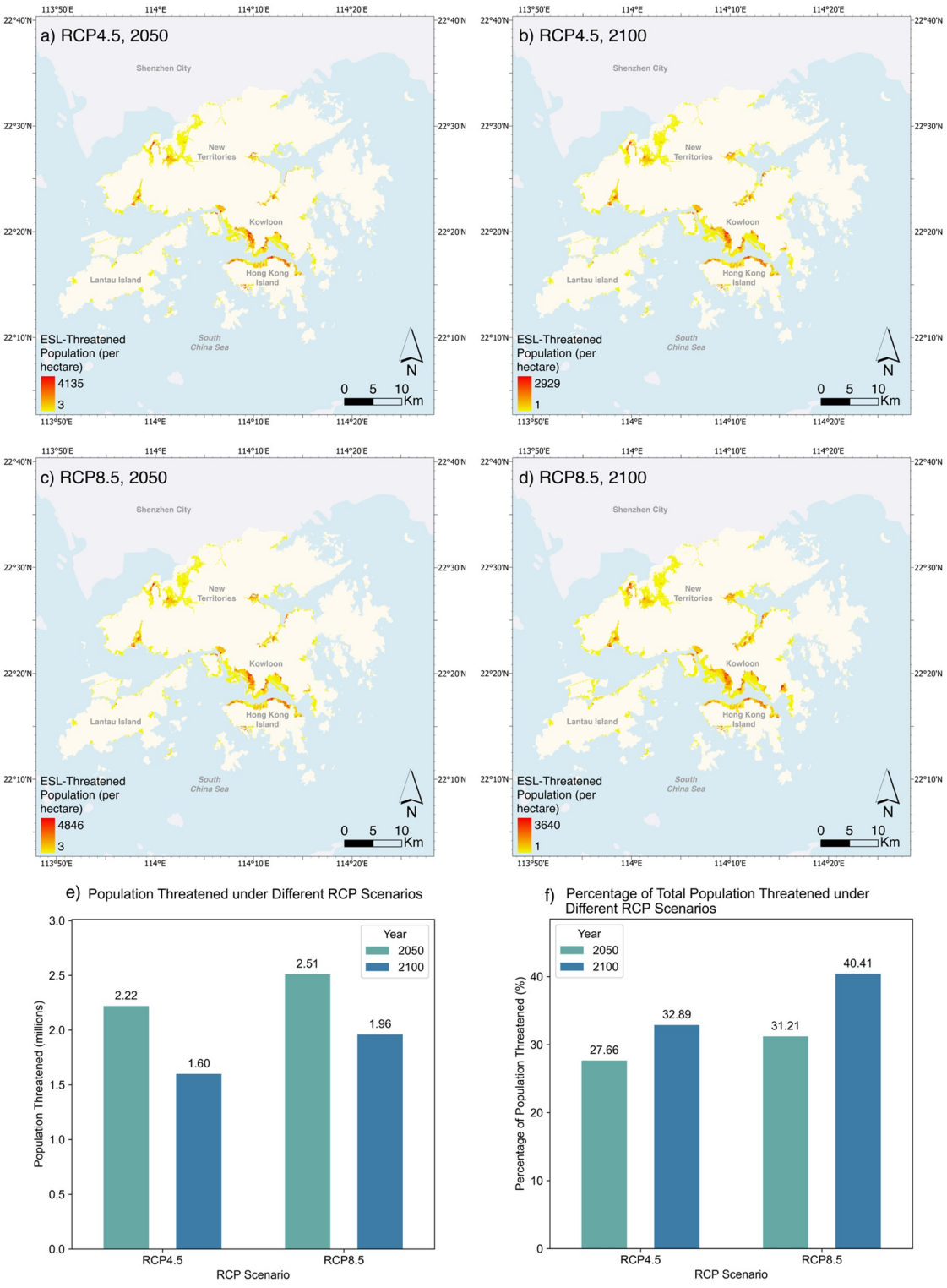


**Fig. 4**. (**a**-**d**) Hong Kong's populations exposed to ESL in different scenarios and years; (**e**) Bar chart of quantities of ESL-threatened population; (**f**) Bar chart of percentages of ESL-threatened population. The maps were created using ArcGIS Pro V3.4 by ESRI, which can be accessed from https://www.esri.com/en-us/arcgis/products/arcgis-pro/.

from 8.03 million in 2050 to 4.85 million by 2100[26], influencing the ESL exposure dynamics. However, from the change in the percentage of the population at risk from 2050 to 2100, it can still be suggested that the social exposure of ESL may increase in 2100 in a given RCP scenario.

*ESL risks on economic activities*

Figure 5 depicts the projected Gross Domestic Product (GDP) within areas exposed to ESL, employing a 30-arc-second resolution grid. It also exhibits the corresponding statistical data. The GDP used in this study is the projected data by Wang and Sun[27]. To provide a consistent estimation without the influence of varying purchasing power, GDP values are expressed in equivalent to 2005 US Dollar (USD) in the data source[27]. Using 2005 USD as a baseline also ensures comparability with the study by Hallegatte et al., which is detailed in the Discussion section[11]. Under RCP4.5, the ESL-exposed GDP is expected to escalate from 270.50 billion USD in 2050 to 366.61 billion USD by 2100, corresponding to 39.52% and 41.10% of the total GDP in those years, respectively. Under RCP8.5, these values are anticipated to be 371.09 billion USD (40.98%) in 2050 and 589.34 billion USD (47.40%) in 2100.

*ESL risks on infrastructure*

Figure 6 documents the potential risks of ESL on the current infrastructure, which is not projected to change extensively, including roads and buildings within Hong Kong. For road infrastructure, under RCP4.5, 783.65 km (16.09%) of roads are anticipated to be at ESL risks in 2050, with the length rising to 990.43 km (20.34%) by 2100. The RCP8.5 scenario predicts 929.19 km (19.08%) of roads at risk in 2050, increasing to 1,105.87 km (22.71%) in 2100. Concerning building structures, out of 340,754 recorded, 72,849 (21.38%) are projected to be at risk in 2050 under RCP4.5, with the number increasing to 85,536 (25.10%) by 2100. The RCP8.5 projections indicate 82,131 (24.10%) buildings at risk in 2050, with the number rising to 101,748 (29.86%) by 2100.

*Land utilization types threatened by ESLs*

The distribution of present-day land use types, which are projected to remain similar, within ESL risk zones is depicted in Fig. 7, with the composition data presented in Fig. 8. Fishponds (Gai Wais) emerge as the most prevalent land use type within ESL-threatened areas across all RCP-year scenarios. Its share of land at risk is 17.00% and 17.11% in 2050 and 2100 under RCP4.5, respectively. For the RCP8.5 scenarios, the proportions are 17.11% in 2050 and 18.56% in 2100. The second most significant land use type is roads and transport facilities. From 2050 to 2100, its share varies from 11.44 to 14.44% under RCP4.5, and from 13.56 to 17.11% under RCP8.5. Figure 8 also highlights the diversity of land use within ESL-threatened regions. Out of 27 types of land utilization classified by the Planning Department, the ESL-threatened area consists of 26 types, indicating a broad spectrum of potential impacts[28]. Only the land use type of reservoirs is not exposed to ESL threats, as the reservoirs are built on high-rise land, or their construction creates highlands.

Moreover, Table 1 summarizes the key results presented above, providing a comparative overview of the physical and socio-economic exposures to ESL risks across the four RCP-year scenarios.

## Discussion

The analysis revealed a consistent pattern in the risks of ESL, as evidenced by the increasing percentages of land, population, and economic outputs at risk, especially under the higher emission scenario RCP8.5. The magnitude of ESL-related threats is predicted to intensify by 2100 compared to 2050 under identical RCP scenarios. Moreover, the potential for ESL damage is higher under RCP8.5 than under RCP4.5 within the same temporal framework. This trend is intrinsically linked to the variations in ESL amplitude. In terms of scenario difference, higher radiative forcing under RCP8.5 contributes to higher ESL, as outlined by Vousdoukas et al.[2]. Similarly, under the same RCP, an upward trajectory in the median ESL from 2050 to 2100 can be attributed to advancing global warming. Consequently, the higher ESL will exacerbate the scope of coastal flood risks and, by extension, the spectrum of socio-economic exposure.

Regarding the reliability of the results, the economic risk simulation in this study agrees with the projections of the Hong Kong region in the global study provided by Hallegatte et al., while the output of this study is fine-grained and has more details on the local scale[11]. In that earlier study, the GDP exposed to ESL in 2050 was estimated for 136 global cities, including Hong Kong. In the case of a 20 cm rise in MSL, which can be linked to RCP4.5, the ESL-threatened GDP of Hong Kong is projected to be 252.9 billion USD[11]. This value is close to the 270.5 billion USD of GDP exposure in 2050 under RCP4.5, as estimated in our study. Moreover, our study and this earlier study both reveal the same trend of Hong Kong's ESL risk that the socio-economic exposure to ESL may increase in the long term, and under more severe climate change scenarios, the ESL risk will be more significant.

This study also investigated that the ESL-threatened lands will extend toward the inland to a limited degree in 2100, compared to the situation in 2050, referring to Fig. 2. Under RCP4.5, the percentage of ESL-threatened land is projected to expand by 1.27% from 2050 to 2100. Under RCP8.5, the projected change is 2.27%. Compared with the initial areas of ESL-threatened land in 2050, whose average is 8.69% across both scenarios, it can be suggested that, though the ESL risks posed onto the land of Hong Kong have limited increase from 2050 to 2100, the initial risk in 2050 will already have been significant, and ESL will threaten a broad area of coastal low land in Hong Kong. This observation reflects that the current coastal flood control facilities are not resistant to 100-year return period ESL events in 2050, highlighting the need to construct capable marine infrastructure before 2050.

Due to the topographic variability in Hong Kong, the ESL-exposed areas are distributed unevenly across the territory. According to Fig. 2, the study identified that the whole coastline of Hong Kong will be exposed to ESL. On most of the coastline sections, the lands with risk are constrained to those adjacent to the ocean, while in some areas, the ESL-threatened areas extend toward inland and create vast interconnected regions. These

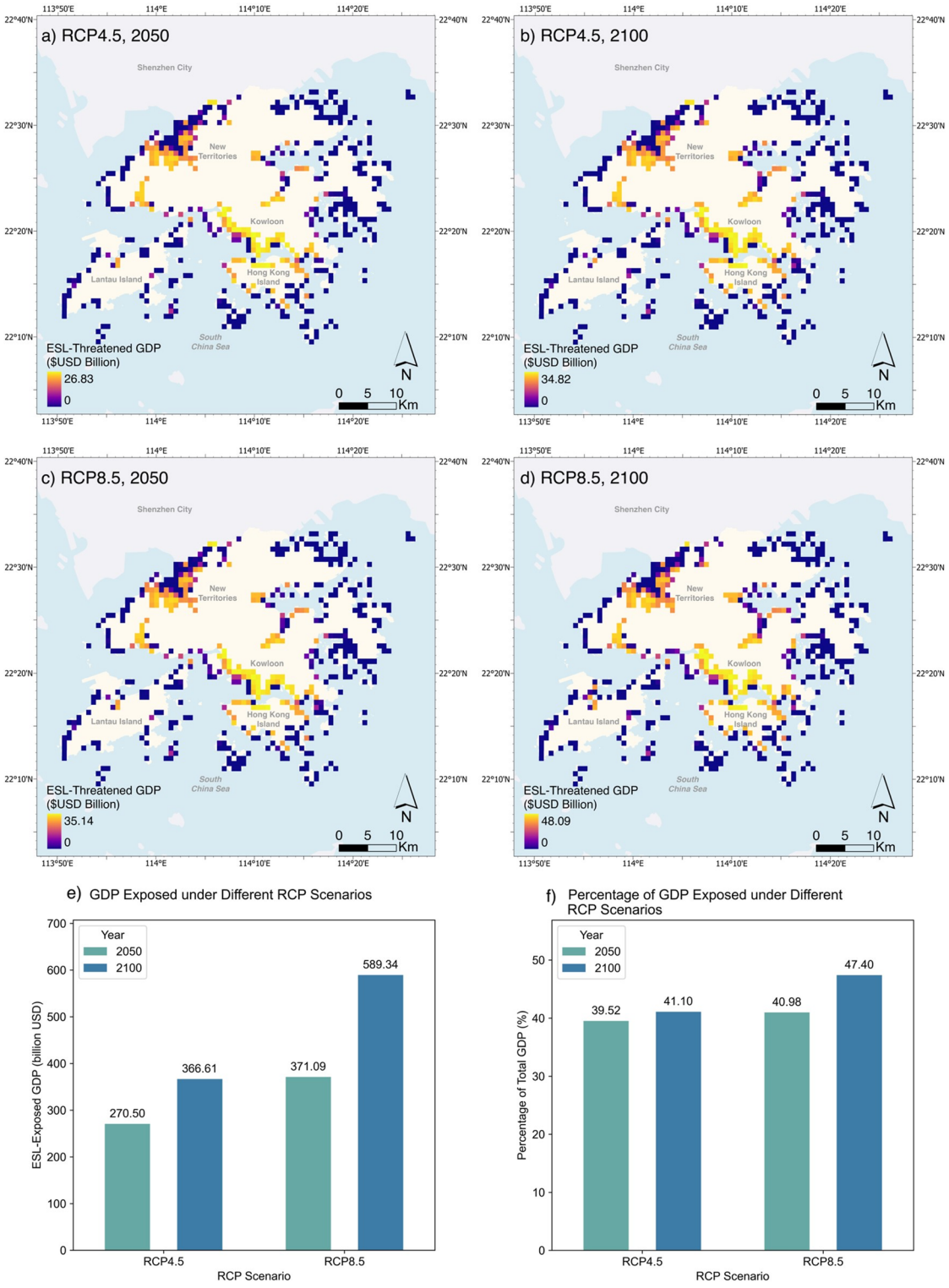


**Fig. 5**. (**a**–**d**) Hong Kong's GDP values exposed to ESL in different scenarios and years; (**e**) Bar chart of GDP values threatened by ESL under different configurations; (**f**) Bar chart of percentages of GDP values threatened by ESL under different configurations. The maps were created using ArcGIS Pro V3.4 by ESRI, which can be accessed from https://www.esri.com/en-us/arcgis/products/arcgis-pro/.

areas mainly include the lands next to the northwestern part of Yuen Long District, Tuen Mun River Estuary, Rambler Channel, Victoria Harbor, Shing Mun River, and Tai Po Waterfront. Figure 9 shows the ESL risks in these regions using the example of RCP8.5. The identified at-risk areas in Yuen Long District, Tuen Mun River, Shing Mun River, and Tai Po Waterfront are consistent with the coastal low-lying or windy residential areas with

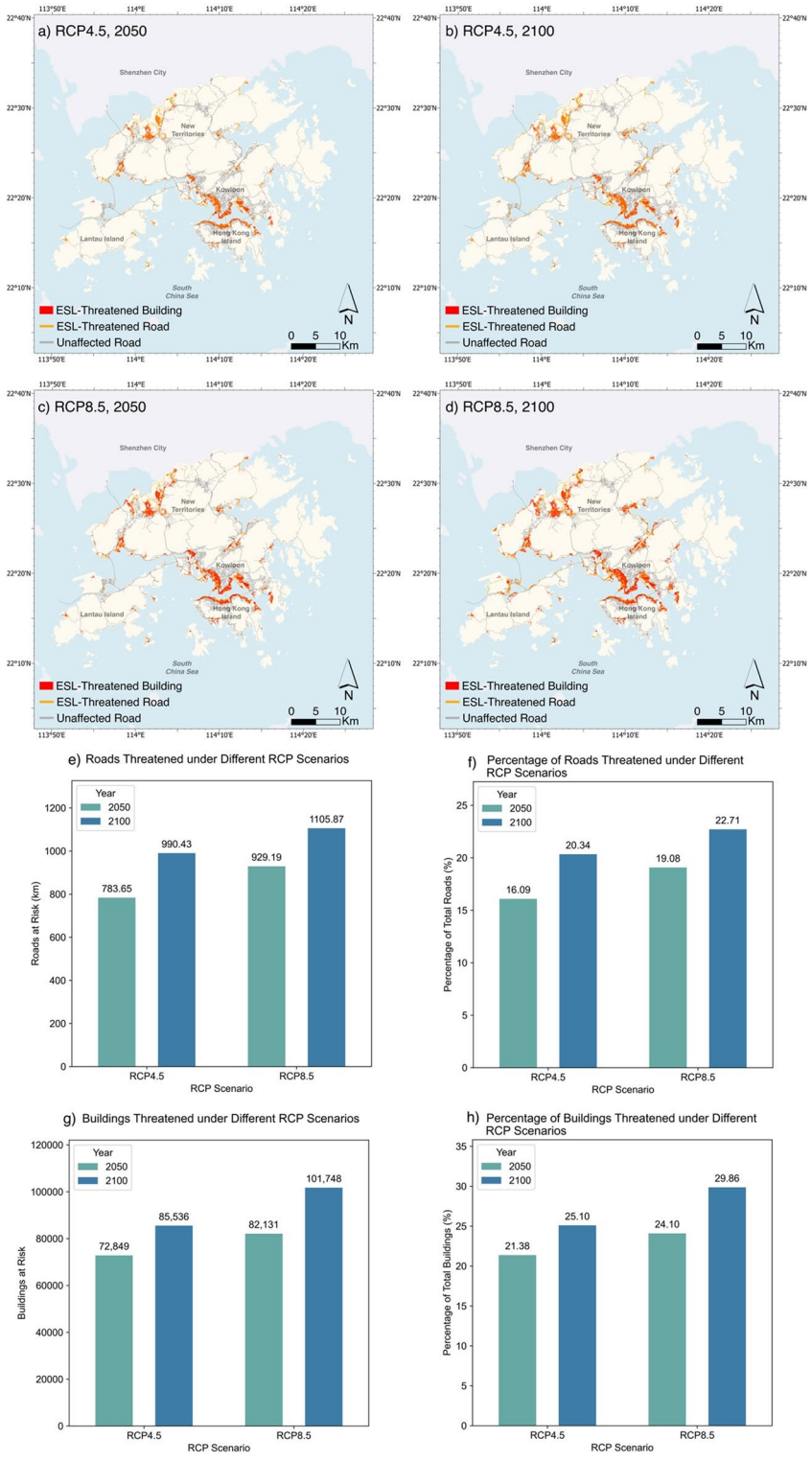


**Fig. 6**. (**a**–**d**) Hong Kong's infrastructure exposed to ESL in different scenarios and years; (**e**–**h**) Bar charts of infrastructure's ESL exposure in Hong Kong in different scenarios and years, presented as quantities and percentages, respectively. The maps were created using ArcGIS Pro V3.4 by ESRI, which can be accessed from https://www.esri.com/en-us/arcgis/products/arcgis-pro/.

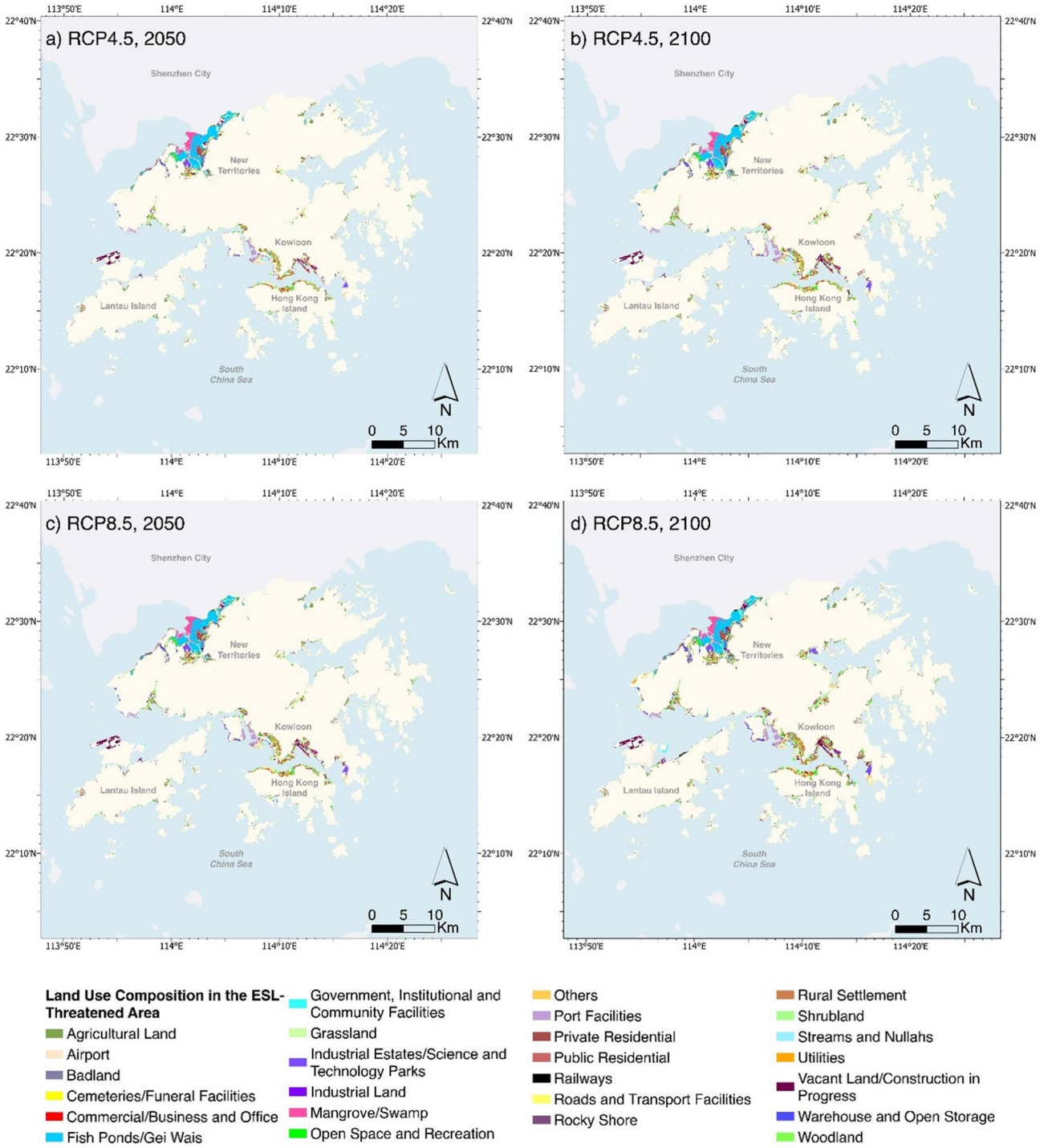


**Fig. 7**. (**a**–**d**) Land use compositions of ESL-threatened lands in Hong Kong in different scenarios and years. The maps were created using ArcGIS Pro V3.4 by ESRI, which can be accessed from https://www.esri.com/en-us/arcgis/products/arcgis-pro/.

high coastal hazard exposure, as defined by the Civil Engineering and Development Department (CEDD)[29]. However, the future ESL risks posed on the lands surrounding the Rambler Channel and Victoria Harbor may be underestimated by CEDD compared to our results[29].

The terrain features can assist in understanding this uneven and segmented spatial distribution of the major ESL-threatened areas. About 75% of Hong Kong's territory is mountainous areas, cutting the coastal flat lowland into discontinuous segments[30]. In addition, the factors leading to the ESL risks of these regions differ. Some of the ESL-threatened locations, including the areas next to Tuen Mun River Estuary, Shing Mun River, and Tai Po Waterfront, are located next to major river estuaries, making them susceptible to the seawater intrusion

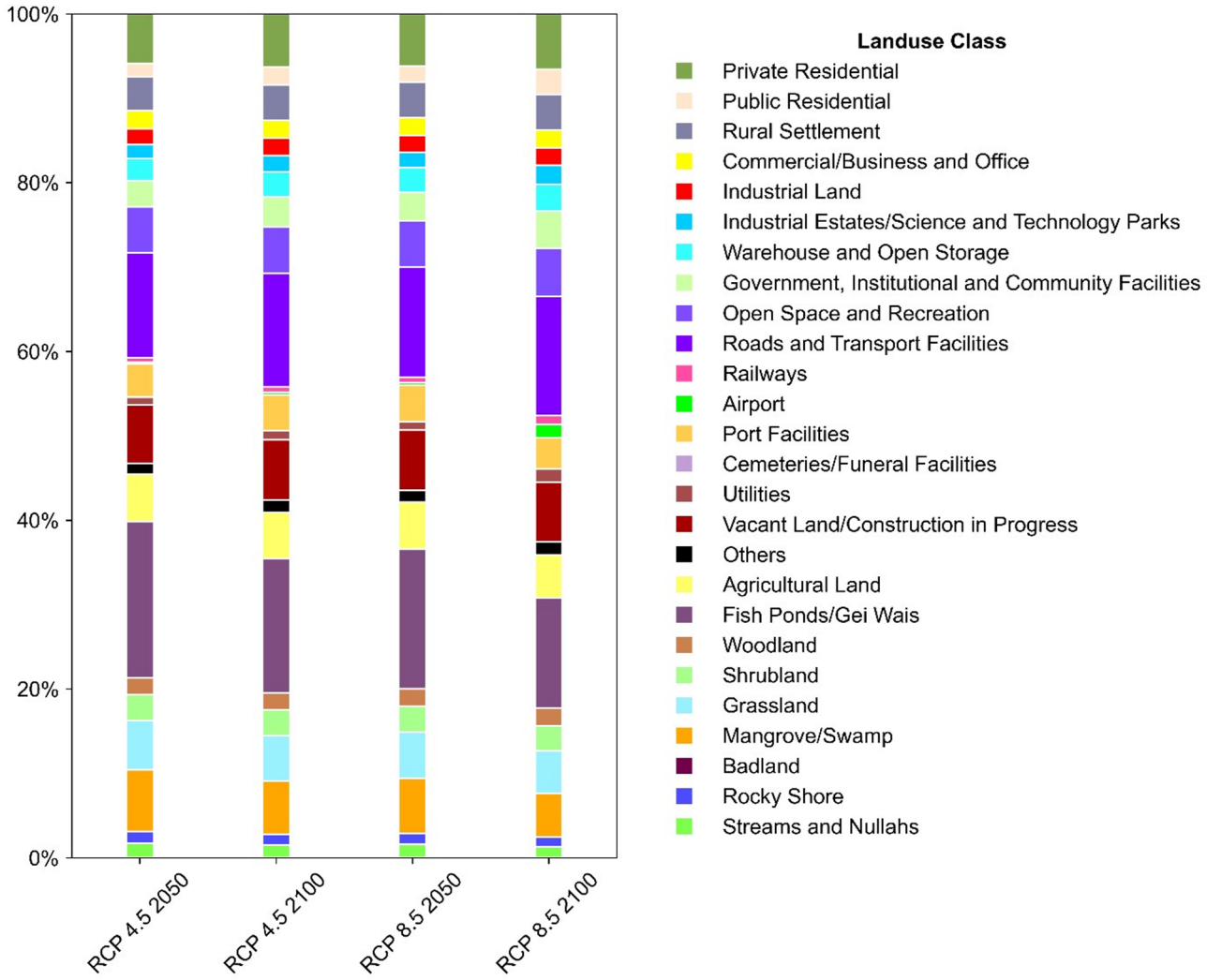


**Fig. 8**. Bar chart of land use compositions of ESL-threatened lands in Hong Kong in different scenarios and years.

| | RCP4.5–2050 | RCP4.5–2100 | RCP8.5–2050 | RCP8.5–2100 |
|---|---|---|---|---|
| Land areas exposed to ESL | 91.68 $km^2$ (8.23%) | 105.83 $km^2$ (9.50%) | 101.82 $km^2$ (9.14%) | 127.11 $km^2$ (11.41%) |
| Average max inundation depth | 1.79 m | 1.90 m | 1.86 m | 2.09 m |
| Population exposed to ESL | 2.22 million (27.66%) | 1.60 million (32.89%) | 2.51 million (31.21%) | 1.96 million (40.41%) |
| GDP exposed to ESL (in 2005 USD Parity) | 270.50 billion USD (39.52%) | 366.61 billion USD (41.10%) | 371.09 billion USD (40.98%) | 589.34 billion USD (47.40%) |
| Road lengths exposed to ESL | 783.65 km (16.09%) | 990.43 km (20.34%) | 929.19 km (19.08%) | 1105.87 km (22.71%) |
| Buildings exposed to ESL | 72,849 (21.38%) | 85,536 (25.10%) | 82,131 (24.10%) | 101,748 (29.86%) |
| Dominant land use types and their shares in ESL zones | Fishponds (17.00%), Roads (11.44%) | Fishponds (17.11%), Roads (14.44%) | Fishponds (17.11%), Roads (13.56%) | Fishponds (18.56%), Roads (17.11%) |

**Table 1**. ESL exposure summary across RCP-year scenarios in Hong Kong.

caused by ESL, as reflected in Fig. 9. In the northwestern part of Yuen Long District, there is a large area of fishponds (Gai Wais) and low-lying wetlands connecting to the ocean, as Fig. 7 reveals. The wide distribution of low-elevation fishponds in the coastal areas of Yuen Long District is also the reason why fishponds are the most prevalent land use type within ESL-threatened areas. The low-lying landform enables potential coastal floods led by ESL to intrude on the inland residential areas and expose a large population to the threats, as reflected in Fig. 4. This area is also highlighted by the governmental coastal hazard report as an area with high vulnerability to multiple coastal risks[29]. Noticeably, the areas neighboring Rambler Channel and Victoria Harbor are not regarded as locations with high coastal hazards by the governmental coastal report. However, this study revealed

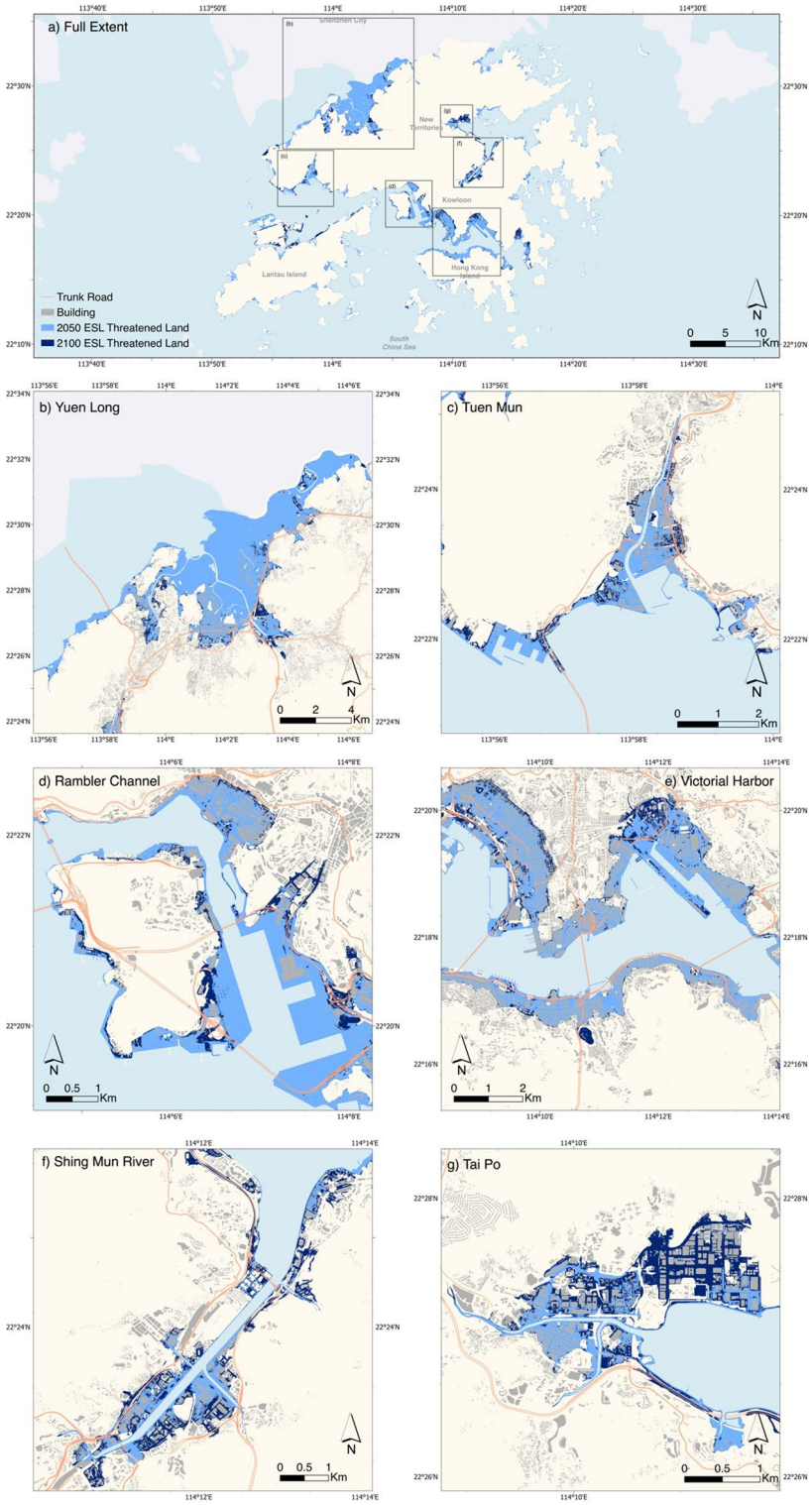


**Fig. 9**. Six major ESL-threatened regions with vast areas at risk, the case of the RCP8.5 scenario. (**a**) Northwestern Yuen Long; (**b**) Tuen Mun River Estuary; (**c**) Rambler Channel Coast; (**d**) Victoria Harbor Coast; (**e**) Areas neighboring Shing Mun River; (**f**) Tai Po Waterfront. The maps were created using ArcGIS Pro V3.4 by ESRI, which can be accessed from https://www.esri.com/en-us/arcgis/products/arcgis-pro/.

that, by 2050, these areas may still have risks of being flooded by ESLs. As most land in these areas was acquired from land reclamation projects[31], one possible reason for their ESL exposure is that the designed elevations of the reclaimed land did not take the long-term ESL into consideration, making the coastal infrastructure not high enough to resist future ESL. Moreover, Sun et al. discovered noticeable coastal reclamation subsidence, which may contribute to higher relative sea level and lead to higher ESL risks in these locations[32].

It should be noted that these identified areas are salient cases that reflect the study's ability to reveal local-scale ESL risks in Hong Kong. Other coastal areas of Hong Kong may also be exposed to future ESL, as shown in Fig. 2. Furthermore, while multiple factors may jointly influence ESL risks at a given location, the analysis in the above paragraph focuses on the primary contributing factors for the identified areas. Additional drivers may also play supplementary roles in these cases. Similarly, other unmentioned coastal locations are likely subject to ESL risks shaped by combinations of the aforementioned factors.

One noteworthy pattern of ESL risks is the disparities between the proportion of ESL-threatened land area and the corresponding percentage of ESL-exposed socio-economic factors. As Fig. 2 reflects, the percentages of land areas projected to be exposed to ESL range from 8.23% to 11.41%. In comparison, the range of ESL-threatened populations is from 27.66 to 40.41%, and the corresponding GDP at risk varies between 39.52 and 47.40%. Namely, the proportions of ESL-exposed population and GDP values are three to four times higher than the percentage of ESL-threatened land area in the same RCP-year configuration. Additionally, the portion of infrastructure exposed to ESL is two times more than that of the ESL-exposed areas in the same configuration, as shown in Figs. 2 and 6. These disparities imply that Hong Kong's socioeconomic exposure to ESL may be amplified compared with the extent of the ESL-exposed territory. The amplification effect can be attributed to the lowland-oriented clustering of population and economic activities and coastal-ward land reclamation in Hong Kong. As existing studies suggest, most of the built areas of Hong Kong are located on low-lying land[3,24], making them susceptible to coastal floods. The coastal land reclamation projects may also expose more population and economic activities to the threats of ESL[32]. These factors jointly amplify the socio-economic risks of future ESL in Hong Kong. This investigation is also consistent with the findings of Wolff et al. that coastal urban area expansion exacerbates social exposure to coastal hazards[12].

In addition, the magnified socio-economic risks of ESL are distributed unevenly across Hong Kong's territory. The contributors are the uneven dispersion of the ESL-threatened land and the clustering of the socio-economic elements. From Fig. 4, it can be suggested that the majority of the ESL-exposed population resides in northwestern Yuen Long, the Tuen Mun River Estuary, and the coast zones of Victoria Harbor and Rambler Channel. Figures 5 and 6 further suggest that the GDP values and infrastructure exposed to ESL mainly cluster on the Victoria Harbor coast. These results reinforce the urgency to build resilient infrastructure in these coastal low-lying zones to protect the dense population, economic activities, and infrastructure highly exposed to future ESL events.

In response to the significant ESL risks identified in our study, we recommend strategic consolidation of infrastructure and policy initiatives. Implementing adaptive infrastructure, such as modular flood barriers that can be adjusted according to updated climate data and projections, can be an effective method[33]. Areas with high ESL risks require reinforced flood defenses, including elevated platforms and robust floodwalls, to mitigate potential damage from ESL events. These approaches were also proposed by the report by CEDD[29].

Additionally, integrating economic incentives, such as tax breaks for businesses implementing flood-proofing measures and the issuance of resilience bonds, may mobilize necessary capital for infrastructure projects to enhance flood defenses. Educational programs that focus on ESL preparedness and engage local populations in resilience-building measures can also be proposed to improve community resilience. For example, the Drainage Services Department provides outreach educational programs to help junior students build resilience under climate change[34]. This type of program can communicate the specific risks to their communities and promote active participation in mitigation efforts.

In terms of limitations, the flood inundation explored in this study only reflects the influence of ESL without considering rainfall or streamflow. The modeling process employed in this study is also oversimplified to enhance computational efficiency, which may not capture all intricacies of flood dynamics. Additionally, the data used to evaluate socioeconomic risks of ESL is sourced from multiple projections, introducing aggregated error into the final output. These limitations underscore the need for more sophisticated approaches to achieve higher quality and accuracy in ESL-threatened area identification.

Addressing these limitations requires developing more complex flood models that incorporate dynamic elements, such as flood durations, and compound floods where ESL, precipitation, and streamflow interact with each other[35]. These models can improve the accuracy and completeness of hazard assessments, especially in terrains where typhoon-induced rainfall significantly impacts coastal areas[36]. Furthermore, integrating regular updates into topographic data and estimating vertical land motion changes will enhance the relevance and precision of future ESL risk projections[37]. Advances in predicting shoreline changes and long-term erosion due to sea level rise and storms should also be considered to refine coastal hazard projections[38]. A systematic approach to monitoring and adjusting policies based on the effectiveness of implemented measures will be important. An accurate and complete coastal flood analysis will further empower urban and economic systems to build resilience against escalating climate challenges.

## Methods

### Study area

The study area covers the whole territory of the Hong Kong Special Administrative Region, China. Figure 1 shows the basic geographical information for the study area. It is located on the southern coast of China, neighboring Shenzhen city to the north and the South China Sea to the south, with a land area of 1114.57 $km^2$ and a sea area of 1640.40 $km^2$[30]. Its territory mainly consists of Hong Kong Island, Kowloon, New Territory, Lantau Island,

and other small islands. Hong Kong is a coastal megacity with a population of about 7.5 million and a GDP of 2818 billion Hong Kong Dollars (HKD) in 2022. As shown in the elevation data in Fig. 1, Hong Kong's terrain is mountainous, constraining urban development in the low-lying areas, especially the coastal zones.

## Data collection and preprocessing

*DTM of Hong Kong*

To capture the topographic conditions in Hong Kong, the study utilized the Digital Terrain Model (DTM) generated from territory-wide airborne Light Detection and Ranging (LiDAR) data, as shown in Fig. 1. It was collected from December 2019 to February 2020 by the CEDD, with additional surveys conducted using Unmanned Aerial System (UAS) LiDAR from December 2020 to February 2021 for areas with problematic data[39]. The DTM data, validated and calibrated by CEDD, is structured within the Hong Kong 1980 Grid System and adheres to the Hong Kong Principal Datum. The DTM's horizontal spatial resolution stands at 0.5 m × 0.5 m, with pixel values represented as 32-bit floats. CEDD has pre-processed it to ensure the exclusion of buildings, bridges, and vegetation. This high-resolution DTM data surpasses the spatial resolution of prior global-scale studies by accurately depicting coastal and marine infrastructure as well as subtle topographic variations, enabling a granular analysis of ESL risks. Furthermore, the DTM's resolution exceeds that of the open-source 30 m global DTM dataset, facilitating building-scale and road-scale analysis of flood exposure, which was unattainable with previous datasets.

Hydrological conditioning is necessary for running flood models on DTM data. Typically, DTM data solely encompasses elevation data on terrestrial surfaces. However, floods led by ESLs can permeate subways and other subterranean facilities, emerging on the opposite side, thereby expanding the risk areas. Thus, hydrological conditioning is essential to process the DTM data and integrate underground features. The spatial data for Hong Kong's underpass and subway systems, provided by the Highways Department of Hong Kong, was utilized for this purpose[40]. Provided by the Common Spatial Data Infrastructure platform, each underpass or subway feature was cataloged as a polyline feature. When integrated into the DTM, their elevation was approximated based on the mean elevation of the two endpoints, a method adapted from the work of Balstrom and Kirby and validated through their case study in the Copenhagen Area[18]. The hydro-conditioned data was stored as raster data without changing its resolution.

*ESL projections*

The study adopted the multi-scenario probability projections for a 100-year return period ESL calculated by Vousdoukas et al. to retrieve the estimated future ESL heights[2]. This return period suits the context of Hong Kong because the 100-year return period ESL event is frequently used as a reference threshold for the planning and construction of coastal flood prevention infrastructure[29]. The projections integrated three components of ESL, including the mean sea level (MSL), the astronomical high tide elevation ($\eta_{\mathrm{tide}}$), and the additional height from waves and storm surges induced by climate extremes ($\eta_{\mathrm{CE}}$). As climate change raises uncertainty, the projections considered various scenarios to evaluate these components. The scenarios were presented by different Representative Concentration Pathways (RCPs). RCPs draft different greenhouse gas concentration trajectories to project the impact of these emissions on climate change[41]. It helps in understanding how varying levels of greenhouse gas concentration will affect the global climate system, ranging from low (RCP2.6) to high (RCP8.5) concentration scenarios, thereby guiding policy and mitigation strategies. These pathways can provide background parameters for ESL projections and facilitate multi-scenario analysis[17].

In the dataset used in this study, the three components (MSL, $\eta_{\mathrm{tide}}$, and $\eta_{\mathrm{CE}}$) were combined to simulate ESL heights for both RCP4.5 (medium greenhouse gas concentration resulting from moderate emission reduction policy) and RCP8.5 (high greenhouse gas concentration resulting from no emission reduction policy), spanning from 2015 to 2100. Due to the availability of ESL projections only under RCP4.5 and RCP8.5 in the dataset by Vousdoukas et al., our analysis is confined to these scenarios[2]. Furthermore, considering the limited feasibility of RCP2.6 under current emission trends and the broader comparative insights offered by the divergence between RCP4.5 and RCP8.5, we focus on these two scenarios to effectively assess the range of potential future risks[41]. Regarding MSL, the projections incorporated various global and local sea level components to forecast a series of MSL changes for each RCP scenario. Following this, $\eta_{\mathrm{tide}}$ projections were formulated based on historical higher high tide records, alongside considerations of the potential impact of sea level rise on tidal heights. The physical parameters for each RCP were then input to the DFLOW FM model and WW3 model to calculate the storm surge and wave height, which were subsequently merged to formulate the projected $\eta_{\mathrm{CE}}$. The study of Vousdoukas et al. utilized Monte Carlo simulations to amalgamate these components, yielding probabilistic forecasts of ESL at 5,000 sample points along the global coastline[2]. The baselines of these final ESL values were rooted in the average local MSL data from 1980 to 2014. The conceptual projection model is explained in Eq. 1.

$$\mathrm{ESL} = \mathrm{MSL} + \eta_{\mathrm{tide}} + \eta_{\mathrm{CE}} \tag{1}$$

The projected ESL data was presented in a probabilistic format, delineating intervals with the median, the 5th percentile, and the 95th percentile for each scenario at decade intervals. To model the ESL-threatened land area for each scenario, only one single ESL value can be input. Therefore, the study opted for the median value for each projection scenario, drawing upon the estimation methodology employed by Sanders et al.[1]. As for time, the project selected 2050 and 2100 to provide a reference for both mid-term and long-term situations of ESL threats.

Furthermore, based on the results from Vousdoukas et al., among the 5000 sample points, this study selected a specific point adjacent to Quarry Bay to represent the ESL scenario for Hong Kong[2]. The point of Quarry Bay is shown in Fig. 1. The Quarry Bay tide gauge has historically been used to represent the MSL of Hong Kong. The

ESL evaluation work by Fang et al. also chose this point to represent Hong Kong's sea level conditions[42]. Thus, it is reasonable to use the ESL data from the same place as an approximation of the whole of Hong Kong's coastline.

Notably, the ESL data's baseline is the local MSL from 1980 to 2014, while the topographic data used in this study applied the Hong Kong Principal Datum. Thus, the baselines of the two datasets should be aligned to conduct flood modeling. As the ESL projection data and the historical MSL of Hong Kong both refer to the waters in Quarry Bay, there is a linear correlation between the MSL component of the ESL and the Quarry Bay historical MSL[43]. Additionally, the MSL from 1980 to 2014 is 1.423 m above the Hong Kong Chart Datum, which is 0.146 m below the Hong Kong Principal Datum[43]. Therefore, the study employed Eq. 2 to convert the projected ESL median ($\mathrm{ESL}_{\mathrm{projected}}$) into the ESL value applicable to the DTM data ($\mathrm{ESL}_{\mathrm{converted}}$). In this equation, $\mathrm{h}_{\mathrm{MSL\ to\ Chart\ Datum}}$ refers to the height of Hong Kong's MSL from 1980 to 2014 relative to Hong Kong Chart Datum, which is 1.423 m, and $\mathrm{h}_{\mathrm{Chart\ Datum\ to\ Principle\ Datum}}$ refers to the height difference between Hong Kong Chart Datum and Hong Kong Principal Datum, which is − 0.146 m. Thus, the baseline of the ESL dataset is converted to the Hong Kong Principal Datum.

$$\mathrm{ESL}_{\mathrm{converted}} = \mathrm{h}_{\mathrm{MSL\ to\ Chart\ Datum}} + \mathrm{h}_{\mathrm{Chart\ Datum\ to\ Principle\ Datum}} + \mathrm{ESL}_{\mathrm{projected}} \tag{2}$$

*Coastline data*

The coastline of Hong Kong was used to set the inflow boundary when running the model. The processing of Hong Kong's coastline data entailed converting the coastline vector to a raster format matching the DTM's pixel size, with grid alignment to the Hong Kong 1980 Grid System utilized by the DTM. This step ensured the coastline's alignment with the DTM data, facilitating more accurate flood modeling.

Hong Kong's coastline data was extracted from the digital topographic map of Hong Kong, which is provided by the Lands Department and can be found on the Hong Kong Common Spatial Data Infrastructure (CSDI) platform[44]. Compared with the open-source Hong Kong administrative boundary, the extracted coastline excludes land borders adjacent to Shenzhen and retains only the water-defined boundary. Additionally, it has less geometric simplification, making it more suitable for being processed along with the high-resolution DTM of Hong Kong.

*Socio-economic data*

The acquisition of pertinent spatial datasets is necessary for the comprehensive analysis of the multifactorial threats of future ESLs. Given the forward-looking nature of this study, it is preferable for the socioeconomic datasets to be projections. Regarding population data, this research selects the 100-m-resolution gridded population dataset of Hong Kong for the year 2020, developed by Bondarenko et al.[45]. This dataset, derived from the Built-Settlement Growth Model (BSGM) and adjusted according to global population estimates from the United Nations Procurement Division (UNPD), is accessible via the WorldPop Hub. However, as this dataset documents only the population distribution for 2020, it lacks future projections. This limitation, thus, required the integration of population forecasts for Hong Kong from 2050 to 2100 by the United Nations[26]. Combining these two sources, the study posited that the spatial distribution of Hong Kong's population will remain largely unchanged from 2020 to 2100. This assumption was grounded in the observed deceleration of urban area growth in Hong Kong since the 2000s and the minimal increase in built-up area, as Li et al. reported[46]. The limited growth of impervious areas (approximately 0.63% of growth from 2004 to 2015) was also observed by Wong et al.[31]. This trend suggests a future limitation in the expansion of residential areas, thus likely stabilizing population distribution patterns. Under this premise, the study assumed that the proportion of the population within each pixel in the 2020 gridded population dataset ($\mathrm{N}_{2020\mathrm{i}}$) could serve as a basis for estimating future population distributions. Consequently, the population for a given year a (a = 2050 or 2100) within a corresponding pixel ($\mathrm{N}_{\mathrm{ai}}$) was calculated using Eq. 3. This assumption facilitated the analysis of at-risk populations due to future ESL events.

$$\mathrm{N}_{\mathrm{ai}} = \sum \mathrm{N}_{\mathrm{ai}} \times \left( \frac{\mathrm{N}_{2020\mathrm{i}}}{\sum \mathrm{N}_{2020\mathrm{i}}} \right) \tag{3}$$

The economic exposure analysis employed a gridded GDP dataset developed by Wang and Sun, featuring 30-arc-second spatial resolution[27]. This dataset offers multi-scenario GDP projections from 2050 to 2100 using the LitPop method, with GDP values represented equal to the US Dollar (USD) value in 2005. Despite its lower spatial resolution, it provided multi-scenario projections aligned with the multi-RCP ESL modeling. Hence, it was selected over other higher-resolution datasets that lacked projected values. The selected scenarios from this dataset utilized shared socioeconomic pathways (SSPs), which were constructed based on RCPs, to depict future conditions[27]. Our study linked the projected GDP under SSP2-4.5 with ESL projections under RCP4.5 and, similarly, GDP under SSP5-8.5 with ESL under RCP8.5 for scenario-aligned subsequent evaluations.

To assess the infrastructure exposed to ESL risks, this study incorporated open-source spatial datasets for roads and permanent buildings provided by the Lands Department on the CSDI platform[47]. Given the anticipated limited built-area expansion, current-year infrastructure data was deemed representative of the future, thus serving as a proxy for assessing the exposure of these artificial structures to future ESL.

Land use data for this analysis was sourced from the CSDI platform and provided by Hong Kong's Planning Department[28]. It detailed the land utilization in 2022 in a 10-m-resolution raster format. This data, derived from space-borne remote sensing and validated by on-site governmental data, was utilized to infer the future land use scenario in Hong Kong because, as mentioned, Hong Kong's built area expansion is limited, constraining the land use changes.

### Identifying areas exposed to ESL risks

The study employed a GIS-based coastal flood inundation model, which integrates pre-processed DTM data with projected ESL heights. It simulates potential inundation areas based on gravity and hydrological connectivity to the coast. This modeling technique is widely recognized in related research domains[13,14,18,48]. It simplifies traditional hydrodynamic models by focusing solely on the end state and the maximal area threatened by coastal floods, omitting temporal details. Despite this simplification, the method offers significant time efficiency and does not necessitate advanced computing resources, as Balstrom and Kirby noted[18]. This efficiency is particularly advantageous when processing extensive study areas with high spatial resolution, which requires substantial data volumes. More importantly, when the simulation time is long enough, the gravity model will share similar results with a full hydrological model[36]. In this study, the simulation time will be longer than 24 h, as ESL events are simulated in the whole territory of Hong Kong, which can be regarded as a long simulation time.

The simulation process assumed a static coastline and uniform sediment transport. It required the hydrologically conditioned DTM, the coastline data, and the ESL height as inputs. The outputs include areas at risk from ESL in both vector and raster formats, with the possible maximum inundation depth in each pixel in the ESL-threatened area in raster format. The model presumed that coastline pixels acted as a continuous source of floodwater caused by ESL, allowing water to penetrate inland to the maximum feasible extent. The potential maximum inundation depth ($d_{max}$) for each at-risk pixel is calculated using Eq. 4. The inundation depth information for the at-risk area was presented in raster format.

$$d_{max} = h_{ESL} - h_{DTM} \tag{4}$$

Considering the selection of ESL projections for both RCP4.5 and RCP8.5 and the temporal markers of 2050 and 2100 for each scenario, the modeling of ESL-threatened areas was executed four times, each with distinct ESL inputs corresponding to the specified RCP-year configuration.

### Assessing socio-economic risks

The risk analysis segment focused on evaluating the potential socio-economic repercussions of future ESL events, spanning four key dimensions: population, economic activities, infrastructure, and land use types. For the population dimension, the analysis explored both the number and the percentage of the Hong Kong population exposed to future ESL threats. Regarding economic activities, the study compiled the value and the proportion of Hong Kong's Gross Domestic Product (GDP) at risk from ESL. Infrastructure analysis encompassed the evaluation of the length of roads, the number of buildings, and their respective proportions exposed to ESL. Lastly, for land use, the study calculated the proportion of each land use category within the ESL-threatened areas and identified the predominant land use type in these areas.

The methodology for analyzing the socio-economic risks of ESL contained two phases. In the first phase, the ESL-threatened zones derived from the above process were used as spatial masks to extract exposed socio-economic features using standard geoprocessing tools. For population exposure assessment, raster layers representing projected distributions for 2050 and 2100, generated as described in Section "Socio-economic data", were clipped using the respective ESL extents under RCP4.5 and RCP8.5. This was implemented using the Raster Clip tool, followed by the Zonal Statistics function to compute the total population exposed within each ESL zone. To visualize the population exposure, a 100 m-resolution raster format with each grid cell reflecting its population count was employed for each scenario. The potential economic risks of ESL were gauged using gridded GDP data.

Economic exposure was assessed through the overlay of projected GDP rasters and ESL-threatened zones. Each GDP layer, aligned to its corresponding RCP and year scenario, was processed identically using raster clipping, and summed using raster algebra to yield total GDP at risk per scenario. The results were also visualized as 30-arc-second-resolution raster layers.

Vector datasets were used for infrastructure and land use analysis. Road and building layers were intersected with ESL-threatened land polygons using the clip tool to isolate ESL-exposed features. The Calculate Geometry function was then used to quantify road lengths and count building footprints at risk. As for the land use raster, ESL zones were used as masks to extract the land use types and their corresponding areas within threatened areas.

In the second phase, the extracted ESL-threatened socio-economic layers were processed using spatial descriptive statistical analysis to quantify the ESL-exposed elements and their relative proportions to the total values of each element. Furthermore, representative high-risk zones were manually selected based on the concentration of exposure and evaluated through a combination of map inspection and contextual interpretation. Thereby, the analysis can provide a localized understanding of the potential socio-economic consequences of future ESL events.

## Data availability

The future extreme sea level (ESL) projection dataset provided by Vousdoukas et al. is freely downloadable on the Joint Research Centre Data Catalogue of the European Commission at https://data.jrc.ec.europa.eu/dataset/jrc-liscoast-10012. The digital terrain model (DTM) of Hong Kong provided by the Civil Engineering and Development Department of Hong Kong is available for download from the Spatial Data Portal at https://sdportal.cedd.gov.hk/#/en/. The subway and underpass data for hydro-conditioning provided by the Highways Department of Hong Kong, the map for extracting coastline, the building and roads data of Hong Kong, and the 2022 Land Utilization Raster are all available on Hong Kong Common Spatial Data Infrastructure (CSDI) Portal at https://portal.csdi.gov.hk/csdi-webpage/. The gridded GDP projection dataset created by Wang and Sun can be downloaded from Zenodo at https://zenodo.org/records/5,880,037. The 2020 gridded population data of

Hong Kong can be downloaded from Worldpop at https://hub.worldpop.org/geodata/summary?id = 49,989. The future population projection provided by the United Nations is free to view on World Population Prospects 2022 at https://population.un.org/wpp/.

Received: 9 March 2025; Accepted: 26 June 2025
Published online: 07 July 2025

## References

1. Sanders, B. F. et al. Large and inequitable flood risks in Los Angeles. *California. Nat. Sustain.* **6**(1), 47–57. https://doi.org/10.1038/s41893-022-00977-7 (2023).
2. Vousdoukas, M. et al. Global probabilistic projections of extreme sea levels show intensification of coastal flood hazard. *Nat. Commun.* **9**, 2360. https://doi.org/10.1038/s41467-018-04692-w (2018).
3. Lai, Y. et al. Compound floods in Hong Kong: Hazards, triggers, and socio-economic consequences. *J. Hydrol. Reg. Stud.* **46**, 101321. https://doi.org/10.1016/j.ejrh.2023.101321 (2023).
4. Lan, C. et al. Assessing indirect impacts of extreme sea level flooding on critical infrastructure. *J. Mar. Sci. Eng.* **11**(7), 1420. https://doi.org/10.3390/jmse11071420 (2023).
5. Wei, S. et al. Coastal urbanization may indirectly positively impact growth of mangrove forests. *Commun. Earth Environ.* **5**(1), 608. https://doi.org/10.1038/s43247-024-01776-y (2024).
6. Rashid, M. M., Moftakhari, H. & Moradkhani, H. Stochastic simulation of storm surge extremes along the contiguous United States coastlines using the max-stable process. *Commun. Earth Environ.* https://doi.org/10.1038/s43247-024-01206-z (2024).
7. Marcos, M., Calafat, F. M., Berihuete, A. & Dangendorf, S. Long-term variations in global sea level extremes. *J. Geophys. Res. Oceans* **120**(12), 8115–8134. https://doi.org/10.1002/2015JC011173 (2015).
8. Menéndez, M. & Woodworth, P. L. Changes in extreme high water levels based on a quasi-global tide-gauge data set. *J. Geophys. Res. Oceans.* https://doi.org/10.1029/2009JC005997 (2010).
9. Sweet, W. V. & Park, J. From the extreme to the mean: Acceleration and tipping points of coastal inundation from sea level rise. *Earth's Future* **2**(12), 579–600. https://doi.org/10.1002/2014EF000272 (2014).
10. Liang, X. et al. Time-frequency analysis framework for understanding non-stationary and multi-scale characteristics of sea-level dynamics. *Front. Mar. Sci.* **9**, 1070727. https://doi.org/10.3389/fmars.2022.1070727 (2023).
11. Hallegatte, S., Green, C., Nicholls, R. J. & Corfee-Morlot, J. Future flood losses in major coastal cities. *Nat. Clim. Change* **3**(9), 802–806. https://doi.org/10.1038/NCLIMATE1979 (2013).
12. Wolff, C., Nikoletopoulos, T., Hinkel, J. & Vafeidis, A. T. Future urban development exacerbates coastal exposure in the Mediterranean. *Sci. Rep.* **10**(1), 14420. https://doi.org/10.1038/s41598-020-70928-9 (2020).
13. Jongman, B., Ward, P. J. & Aerts, J. C. J. H. Global exposure to river and coastal flooding: Long term trends and changes. *Glob. Environ. Change* **22**(4), 823–835. https://doi.org/10.1016/j.gloenvcha.2012.07.004 (2012).
14. Muis, S., Verlaan, M., Winsemius, H. C., Aerts, J. C. J. H. & Ward, P. J. A global reanalysis of storm surges and extreme sea levels. *Nat. Commun.* **7**, 11969. https://doi.org/10.1038/ncomms11969 (2016).
15. Wahl, T. et al. Understanding extreme sea levels for broad-scale coastal impact and adaptation analysis. *Nat. Commun.* **8**, 16075. https://doi.org/10.1038/ncomms16075 (2017).
16. Dada, O. A., Angnuureng, D. B., Almar, R. & Morand, P. Linking human perception and scientific coastal flood risk assessment (Anlo Beach Community, Ghana). *Ocean Coast. Manag.* **243**, 106758. https://doi.org/10.1016/j.ocecoaman.2023.106758 (2023).
17. Rasmussen, D. J., Kulp, S., Kopp, R. E., Oppenheimer, M. & Strauss, B. H. Popular extreme sea level metrics can better communicate impacts. *Clim. Change* **170**(3–4), 30. https://doi.org/10.1007/s10584-021-03288-6 (2022).
18. Balstrom, T. & Kirby, J. A GIS-based screening workflow for coastal storm surge impact assessments and mitigation action consideration. *J. Coast. Res.* **38**(4), 712–724. https://doi.org/10.2112/JCOASTRES-D-21-00097.1 (2022).
19. Hallegatte, S. et al. Assessing climate change impacts, sea level rise and storm surge risk in port cities: A case study on Copenhagen. *Clim. Change* **104**(1), 113–137. https://doi.org/10.1007/s10584-010-9978-3 (2011).
20. Zheng, Y., Zhuang, W. & Du, Y. Extreme sea level changes over the tropical western Pacific in 15 °C and 20 °C warmer climates. *Front. Mar. Sci.* **10**, 1130769 (2023).
21. Kato, F. & Tajima, Y. Coastal adaptation to climate change in Japan: A review. *Coastal Eng. J.* **65**, 597–619 (2023).
22. He, Y. H., Mok, H. Y. & Lai, E. S. T. Projection of sea-level change in the vicinity of Hong Kong in the 21st century. *Int. J. Climatol.* **36**(9), 3237–3244. https://doi.org/10.1002/joc.4551 (2016).
23. Tao, S., Hua, Y. & Dong, S. Intensity estimation of extreme meteorological and hydrological factors induced by tropical cyclones affecting Hong Kong. *J. Ocean Univ. China* **22**(2), 313–323. https://doi.org/10.1007/s11802-023-5120-9 (2023).
24. Chui, S. K., Leung, J. K. Y. & Chu, C. K. The development of a comprehensive flood prevention strategy for Hong Kong. *Int. J. River Basin Manag.* **4**(1), 5–15. https://doi.org/10.1080/15715124.2006.9635270 (2006).
25. Zou, F., Tenzer, R., Fok, H. S., Meng, G. & Zhao, Q. The sea-level changes in Hong Kong from tide-gauge records and remote sensing observations over the last seven decades. *IEEE J. Sel. Top. Appl. Earth Obs. Remote Sens.* **14**, 6777–6791. https://doi.org/10.1109/JSTARS.2021.3087263 (2021).
26. United Nations. *World Population Prospects 2022*. https://population.un.org/wpp/ (2022).
27. Wang, T. & Sun, F. Global gridded GDP data set consistent with the shared socioeconomic pathways. *Sci. Data* https://doi.org/10.1038/s41597-022-01300-x (2022).
28. Planning Department. *2022 Raster grids on land utilization*. Hong Kong CSDI Portal. https://portal.csdi.gov.hk/geoportal/?lang=en&datasetId=pland_rcd_1665742315124_26227 (2023).
29. Civil engineering and development department. *Study of coastal hazards under climate change and extreme weather and formulation of improvement measures – feasibility study (Ref. R17–04)*. https://www.cedd.gov.hk/eng/media-corner/project-reports/index-id-24.html (2022).
30. Information services department. *Hong Kong Yearbook 2022*. https://www.yearbook.gov.hk/2022/en/ (2022).
31. Wong, K., Zhang, Y., Tsou, J. Y. & Li, Y. Assessing impervious surface changes in sustainable coastal land use: A case study in Hong Kong. *Sustainability* https://doi.org/10.3390/su9061029 (2017).
32. Sun, Q. et al. Monitoring coastal reclamation subsidence in Hong Kong with distributed scatterer interferometry. *Remote Sens.* **10**(11), 1738. https://doi.org/10.3390/rs10111738 (2018).
33. Sun, L., Qi, Y., Gao, X., Guo, W. & Zhang, N. Stability of supported geomembrane tube flood barriers of novel design. *J. Flood Risk Manag.* **13**, e12574. https://doi.org/10.1111/jfr3.12574 (2020).
34. Drainage services department. *DSD outreach educational programme*. https://www.dsd.gov.hk/EN/Education/DSD_Outreach_Educational_Programme/index.html (2020).
35. Sanders, B. F. & Schubert, J. E. PRIMo: Parallel raster inundation model. *Adv. Water Resour.* **126**, 79–95. https://doi.org/10.1016/j.advwatres.2019.02.007 (2019).
36. Sosa, J., Sampson, C., Smith, A., Neal, J. & Bates, P. A toolbox to quickly prepare flood inundation models for LISFLOOD-FP simulations. *Environ. Model. Softw.* **123**, 104561. https://doi.org/10.1016/j.envsoft.2019.104561 (2020).

37. Nicholls, R. J. et al. A global analysis of subsidence, relative sea-level change and coastal flood exposure. *Nat. Clim. Change* **11**(4), 338–342. https://doi.org/10.1038/s41558-021-00993-z (2021).
38. Passeri, D. L., Hagen, S. C., Bilskie, M. V. & Medeiros, S. C. On the significance of incorporating shoreline changes for evaluating coastal hydrodynamics under sea level rise scenarios. *Nat. Hazards* **75**(2), 1599–1617. https://doi.org/10.1007/s11069-014-1386-y (2015).
39. Civil Engineering and Development Department. *LiDAR data*. Spatial data portal. https://sdportal.cedd.gov.hk/#/en/lidar (n.d.).
40. Highways Department. *Subway and Underpass*. Hong Kong CSDI Portal. https://portal.csdi.gov.hk/geoportal/?lang=en&datasetId=hyd_rcd_1632360923030_42011 (2024).
41. Raftery, A. E., Zimmer, A., Frierson, D. M. W., Startz, R. & Liu, P. Less than 2 °C warming by 2100 unlikely. *Nat. Clim. Change* **7**(9), 637–641. https://doi.org/10.1038/nclimate3352 (2017).
42. Fang, J. et al. Extreme sea levels along coastal China: Uncertainties and implications. *Stoch. Environ. Res. Risk Assess.* **35**(2), 405–418. https://doi.org/10.1007/s00477-020-01964-0 (2021).
43. Lands Department. *Reference Notes on Land Surveying — Control & Mapping* [Brochure]. https://www.hkis.org.hk/ufiles/ref1_0.pdf (1994).
44. Lands Department. *Digital Topographic Map iB1000*. Hong Kong CSDI Portal. https://portal.csdi.gov.hk/geoportal/?lang=en&datasetId=landsd_rcd_1637223748322_25497 (2024).
45. Bondarenko, M., Kerr, D., Sorichetta, A. & Tatem, A. J. Census/projection-disaggregated gridded population datasets, adjusted to match the corresponding UNPD 2020 estimates, for 183 countries in 2020 using Built-Settlement Growth Model (BSGM) outputs. *WorldPop*. https://hub.worldpop.org/geodata/summary?id=49989 (2020).
46. Li, L., Chan, P. W., Wang, D. & Tan, M. Rapid urbanization effect on local climate: Intercomparison of climate trends in Shenzhen and Hong Kong, 1968–2013. *Clim. Res.* **63**(2), 145–155. https://doi.org/10.3354/cr01293 (2015).
47. Lands Department. *Buildings*. Hong Kong CSDI Portal. https://portal.csdi.gov.hk/geoportal/?lang=en&datasetId=landsd_rcd_1637211194312_35158 (2024).
48. Hinkel, J. et al. Coastal flood damage and adaptation costs under 21st century sea-level rise. *Proc. Natl. Acad. Sci. U.S.A.* **111**(9), 3292–3297. https://doi.org/10.1073/pnas.1222469111 (2014).


## Acknowledgements

This study was jointly supported by the National Natural Science Foundation of China (W2412136, 42071390); the Hui Oi-Chow Trust Fund (263690575); the Research Grants Council (RGC) of Hong Kong, China (HKU27602020, HKU17613022); the Croucher Foundation (CAS22902/CAS22HU01), Hong Kong, China; and the Key Laboratory of Spatial Data Mining & Information Sharing of Ministry of Education, Fuzhou University (No. 2023LSDMIS07).

## Author contributions

Z.C. contributed to Conceptualization, Methodology, Software, Formal analysis, Investigation, Data Curation, Writing Original Draft, and Visualization. S.J. contributed to Software, Validation, Investigation, Data Curation, and Visualization X.L. contributed to Conceptualization, Resources, Review, Editing, and Supervision. H.Z. contributed to Resources, Review, Editing, Supervision, Project administration, and Funding acquisition.

## Declarations

## Competing interests

The authors declare no competing interests.

## Additional information

**Correspondence** and requests for materials should be addressed to H.Z.

**Reprints and permissions information** is available at www.nature.com/reprints.

**Publisher's note** Springer Nature remains neutral with regard to jurisdictional claims in published maps and institutional affiliations.